

Proceedings of the Korean Nuclear Society Autumn Meeting
Yongpyung, Korea, 2003

Wavelet Denoising Method: Application to the Flow Rate Estimation for Water Level Control

Gee Young Park*, Jinho Park*, Jung Han Lee*, Bong Soo Kim*, and Poong Hyun Seong**

*: Korea Atomic Energy Research Institute
150 Deokjin-dong, Yuseong-gu,
Daejeon, Korea 305-353

** : Korea Advanced Institute of Science and Technology
373-1 Guseong-dong, Yuseong-gu,
Daejeon, Korea, 305-701

Abstract

The wavelet transform decomposes a signal into time- and frequency-domain signals and it is well known that a noise-corrupted signal could be reconstructed or estimated when a proper denoising method is involved in the wavelet transform. Among the wavelet denoising methods proposed up to now, the wavelets by Mallat and Zhong can reconstruct best the pure transient signal from a highly corrupted signal. But there has been no systematic way of discriminating the original signal from the noise in a dyadic wavelet transform. In this paper, a systematic method is proposed for noise discrimination, which could be implemented easily into a digital system. For demonstrating the potential role of the wavelet denoising method in the nuclear field, this method is applied to the steam or feedwater flow rate estimation of the secondary loop. And the configuration of the S/G water level control system is proposed for incorporating the wavelet denoising method in estimating the flow rate value at low operating powers.

1. Introduction

The wavelet transform maps the time domain signal into the frequency and time domains as the windowed or short time Fourier transform does [1]. The windowed FT has a constant window width across both the time and frequency domains. On the contrary, the widths of the wavelets in the wavelet transform are varied according to the scales. As the scale goes to the high frequency range, the width of the wavelet is reduced over the time domain and also increases over the frequency domain so that the short time and highly oscillating signals can be isolated. When the scale corresponds to the low frequency range in which the signals usually have a long period of time, the width of the wavelet is enlarged over the time domain

and correspondingly, is reduced in the frequency domain [2].

More interestingly, some types of wavelets have the capability of showing that the maximum values of the decomposed signals by the wavelet transform represent the sharp variation points of the signal which are called the singularities and the variations of these maximum values across the scale characterize the type of the singularity [3].

By the use of these wavelets, the variations affected by noise can be differentiated from those due to the signal and the noise signals can be removed significantly when the signal is reconstructed from the selected maximum values of the wavelet transform due to the signal. This method can be applied to the noise removal or reduction of signals related to nuclear power plant operations and, in this paper, it is specifically incorporated into the water level controller for the on-line estimation of the true flow rate under a very high noise environment where the noise signals are twice the magnitude of the original signal at low operating powers.

2. Wavelet Transform and Noise Reduction

Mallat and Zhong [3] showed that some types of wavelets have a property that the maximum values of the decomposed signals along the scale represent the sharp variation points of the original signal. Using this wavelet, the signal that approximates the original signal very closely can be recovered from the noise-corrupted signal. The wavelet developed by Mallat and Zhong is the first derivative of some kind of smoothing function and it is not orthogonal. Orthogonal wavelets having the properties described above were proposed by Cvetković and Vetterli [4]. In both wavelets, the decomposition and the synthesis of the signals are performed by the use of the non-subsampled filter banks, which have an advantage of shift invariance compared to the critically sampled octave band filter banks [5]. In this section, the wavelet transform by Mallat and Zhong is described briefly because this wavelet is used in the noise reduction procedures in this paper.

The Hilbert space $L^2(\mathbb{R})$ is defined as the set of square-integrable functions such that

$$\int_{-\infty}^{\infty} |f(x)|^2 dx < \infty, \text{ for all } f(x) \in L^2(\mathbb{R}).$$

The Fourier transform of $f(x)$ is denoted by $\hat{f}(\omega)$. The convolution of the two functions $f(x) \in L^2(\mathbb{R})$ and $g(x) \in L^2(\mathbb{R})$ is represented as

$$f * g(x) = \int_{-\infty}^{\infty} f(u)g(x-u)du,$$

and the dilation of a function $\psi(x)$ by the scale s ($s > 0$) is defined as

$$\psi_s(x) = \frac{1}{s} \psi\left(\frac{x}{s}\right). \quad (1)$$

In this paper, the scale s is restricted to the dyadic scale, i.e., $s = 2^j$ ($j \in \mathbb{Z}$). The wavelet transform of $f(x) \in L^2(\mathbb{R})$ at the scale 2^j and at the position x is defined as

$$W_{2^j} f(x) = f * \psi_{2^j}(x), \quad (2)$$

where $j \in \mathbb{Z}$ and ψ_{2^j} is the dilation of ψ by the scale 2^j as in Eq.(1). In Eq.(2), the function $\psi(x)$ is called the wavelet. The reconstruction or synthesis of $f(x)$ from the wavelet transform of Eq.(2) is defined as

$$f(x) = \sum_{j=-\infty}^{\infty} W_{2^j} f * \chi_{2^j}(x), \quad (3)$$

where $\chi(x)$ is called the reconstruction or synthesis wavelet.

For Eq.(2), the resolution of the dyadic scale 2^j can be from $j = -\infty$ to ∞ . In reality, however, this could never be achieved because we have to treat the finite length of the signal samples, i.e.,

$$D = \{d_0, d_1, \dots, d_{N-1}\}, \quad (4)$$

where N is the number of data samples and is usually the power of 2. We set the finest scale by $s = 1$ and set the coarsest scale by $s = 2^J$ with $J = \log_2(N)$.

At this time, we need to introduce a smoothing function $\phi(x)$ with the frequency response function such as

$$|\hat{\phi}(\omega)|^2 = \sum_{j=1}^{\infty} \hat{\psi}(2^j \omega) \hat{\chi}(2^j \omega), \quad (5)$$

so that the smoothing operation S at the scale of 2^J is defined as

$$S_{2^j} f(x) = f * \phi_{2^j}(x). \quad (6)$$

The smoothing function ϕ in Eq.(5), the wavelet ψ in Eq.(2), and the reconstruction wavelet χ in Eq.(3) are obtained from the infinitely product of an FIR (Finite Impulse Response) filter and the frequency response functions, respectively [3] such that

$$\hat{\phi}(\omega) = e^{-i\omega w} \prod_{p=1}^{\infty} H(2^{-p} \omega), \quad (7a)$$

$$\hat{\psi}(2\omega) = e^{-i\omega w} G(\omega) \hat{\phi}(\omega), \quad (7b)$$

$$\hat{\chi}(2\omega) = e^{-i\omega w} K(\omega) \hat{\phi}(\omega), \quad (7c)$$

where w is a shift constant. The FIR filters $H(\omega)$, $G(\omega)$, and $K(\omega)$ are all 2π periodic functions and $|H(0)| = 1$. By manipulating Eq.(5) and Eqs.(7), the necessary and sufficient condition for the perfect reconstruction can be obtained by

$$|H(\omega)|^2 + G(\omega)K(\omega) = 1.$$

For the discrete-time signal D in Eq.(4), it can be found that there exists a function $f(x) \in L^2(\mathbb{R})$ such that $S_1 f(k) = d_k$, for $k = 0, 1, \dots, N-1$. Then, the set of decomposed signals through the wavelet transform operation \mathbf{W} are generated by

$$\mathbf{W}f = \{W_{2^j} f(k), W_{2^j} f(k), \dots, W_{2^j} f(k), S_{2^j} f(k)\}, \text{ for } k = 0, 1, \dots, N-1. \quad (8)$$

The fact that $\psi(x)$ is the first derivative of a smoothing function implies that $\hat{\psi}(\omega)$ must have a zero of the multiplicity one at $\omega = 0$ [4]. By the proper choice of $H(\omega)$, a wavelet having a single zero at $\omega = 0$ can be designed to be regular and to have a compact support.[3].

The modulus maxima are the values of the decomposed signals at the points determined from the fact that the absolute value of the wavelet transform at a point k is larger than that of the adjacent points along the position with respect to a scale 2^j . And the modulus maxima operator M is defined by

$$M = \{(W_{2^j} f, k) : |W_{2^j} f(k)| \geq |W_{2^j} f(k-1)|, |W_{2^j} f(k)| \geq |W_{2^j} f(k+1)|, j = 1, \dots, J\}. \quad (9)$$

Based on the fact that the modulus maxima in Eq.(9) obtained by the use of Eqs.(7) represent the singularities or the sharp variation points of the signal, one more important and

interesting fact is to be described in order to distinguish the signal from the noise. The absolute value of each decomposed signal in Eq.(8), which also includes the modulus maxima of Eq.(9), can be bounded by

$$|W_{2^j} f(x)| \leq K(2^j)^\alpha, \text{ for } \forall j \text{ and } x \in]a, b[. \quad (10)$$

In Eq.(10), K is a positive constant and α is called the Lipschitz exponent defined such that, for $(x_1, x_2) \in]a, b[$, there exists $K > 0$ such that $|f(x_1) - f(x_2)| \leq K|x_1 - x_2|^\alpha$. If $\alpha > 0$, which usually represents the inflection point of the signal, the modulus maxima increases as the dyadic scale increases ($j \rightarrow J$). On the contrary, when $\alpha < 0$, which corresponds to the effect of the spike-like noise signal, the modulus maxima increase as the scale goes to the finest scale ($j \rightarrow 1$).

This characterization provides a possible way for identifying whether the modulus maxima across the scale at some points are resulted from the noise or the variation of the signal. When the identification process of all the modulus maxima is finished, the modulus maxima from the noise are eliminated leaving only those from the signal.

After removing the noise-induced modulus maxima, the wavelet transform is reconstructed from the remaining modulus maxima over the scale and the decomposed signals by the smoothing operation as in Eq.(6). This reconstruction procedure is performed through the alternating projections of three operators such as

$$P = P_V \circ P_\Gamma \circ P_Y, \quad (11)$$

where P is the projection operator, V is the space of all the dyadic wavelet transforms of the functions in $L^2(\mathbb{R})$, Γ is the space of the sequences that have the same values at the modulus maxima points for all the scales as that obtained by Eq.(9), and Y is the space of the sequences whose values at the points between the two consecutive points of the modulus maxima for any scale are interpolated by the piece-wise exponential functions and that have no or few oscillations between the two adjacent modulus maxima.

At the final stage, the signal is now reconstructed from the so-called inverse wavelet transform of Eq.(3) with the wavelet transform in Eq.(3), which is obtained from Eq.(2), being now replaced with the wavelet transform reconstructed from Eq.(11). In fact, the reconstructed signal is not the original signal but approximates it because the alternating projections of Eq.(11) converge, at most, onto the set that is very close to the set of the wavelet transform of the original pure signal [3].

3. Efficient Denoising Method for Dyadic Wavelet Transform

In this section, a systematic and efficient way of noise discrimination based on the dyadic wavelets described in the previous section is proposed for an arbitrary signal. In fact, Belluzzo, et al [6] performed a study similar to our work. But, the wavelet transform used in their work was not the dyadic wavelet transform. It involved a small value slightly larger than 1 as the scale, which can produce a much denser set of modulus maxima than the dyadic scale so that the positions of the modulus maxima for the signal variations can be separated from those for the noise more accurately with the inevitable pay for much larger burdens of the calculation efforts.

Fig.1 shows the original pure, exponentially decaying, signal with transients around the

center position. The total number of the signal samples is 1024 and it is assumed that the sampling time is 1 sec. Fig.2 shows the signal corrupted by the Gaussian white noise whose maximum value is up to 5. In this test, the maximum scale level J is given by $J = 7$ and the position k of each modulus maxima at the scale 2^j is determined by

$$\{k : |W_{2^j}f(k)| > |W_{2^j}f(k-1)|, |W_{2^j}f(k)| \geq |W_{2^j}f(k+1)|\}.$$

The procedure for removing the modulus maxima due to the noise is as follows. At first, we note that the positions, along the time sequence axis, of the modulus maxima for a pure signal as depicted in Fig.3 where the modulus maxima for all the scales are displayed simultaneously. By carefully inspecting the positions of the modulus maxima corresponding to one of the signal variations numerated by (1)~(7) in Fig.3, one could find the property: Let $\lambda_j(k_j)$ denote the position of one of the modulus maxima at the time k_j and at the scale 2^j . And δ_j is defined as $\delta_j = \lambda_j(k_j) - \lambda_{j+1}(k_{j+1})$, where $\lambda_j(k_j)$ and $\lambda_{j+1}(k_{j+1})$ have the same sign and are very close to each other. From the results of Fig.3, it could be found that $\delta_{j-1} = 0.5\delta_j$.

Based on this property, the selection of the modulus maxima can be performed easily even though the dyadic wavelet transform has a coarser set of modulus maxima than the wavelet transform in the work of Belluzzo, et al [6]. The discrimination of the modulus maxima begins at the coarsest scale 2^J and then, goes up to the next finer scale. At the coarsest scale 2^J , we determined the positions of the modulus maxima $\lambda_j(k_j)$, $k_j = 1, \dots, K_{J,\max}$. This determination can be done easily because almost all of the modulus maxima due to the noise disappear at this maximum scale level of $J = 7$. At the scale $J-1$, the modulus maxima due to the signal variations are determined along the same way as in Belluzzo, et al.

From the scale 2^{J-2} to 2^1 , the modulus maxima are determined by use of the facts that, with the reference value of δ_j calculated by $\delta_j = 0.5\delta_{j+1}$, if both $\lambda_j(k_j)$ and $\lambda_{j+1}(k_{j+1})$ have the same sign and $\lambda_j(k_j)$ is closer to the reference value of $\delta_j + \lambda_{j+1}(k_{j+1})$ than any other λ_j at the same scale 2^j , then $\lambda_j(k_j)$ is involved in the modulus maxima representing a variation point of the signal as indicated by the pre-determined $\lambda_{j+1}(k_{j+1})$, $\lambda_{j+2}(k_{j+2})$, \dots , $\lambda_j(k_j)$.

Fig.4 shows the modulus maxima for the noisy signal samples of Fig.2 and the discrimination results of the modulus maxima are shown in Fig.5. From the results of Fig.5, the wavelet transform that will approximate very closely the wavelet transform of the original pure signal can be reconstructed by the alternating projections. For the alternating projections, the one-by-one alternations of three projection operators are iterated up to 40 times.

The reconstructed or synthesis signal from the inverse wavelet transform based on the reconstructed wavelet transform is shown in Fig.6, together with the original signal. From Fig.6, the noise effect is reduced remarkably and the signal reconstructed in this way approximates the pure signal satisfactorily.

4. Configuration of S/G Water Level Control System

In this section, the wavelet denoising method is incorporated into the water level controller in order for the on-line estimation of the flow rate and a proper configuration of the control system is presented to combine the wavelet transform with the water level controller.

For the existing feedwater control systems for nuclear steam generators, only the water level measurement is used at low operating powers, discarding the measurements of the steam/feedwater flow rates because of the extremely high noise level which is often twice the

level of the actual signal [7].

In this paper, the noise reduction technique by the wavelet transform is applied to the estimation of the steam flow rate. As a water level controller, any feedback control scheme can be employed. The water level controller used in this simulation test is the fuzzy learning controller (FLC) [8]. Though the FLC showed a very good control performance for various simulation tests, it is not desirable that the FLC be implemented into the feedwater control system because the FLC requires accurate information on the mismatch between the feedwater and steam flow rates, as do the other controllers. In the FLC with the wavelet transform, the measurement of the steam flow rate is first fed into the wavelet transform. The wavelet transform recovers the steam flow rate signal and provides this to the flow error calculation module located at the input port of the FLC. An overall schematic diagram of the control structure is depicted in Fig.7.

In Fig.7, the g_l , g_f , and g_o are the normalization factors. The e_l and e_f are the errors defined as $e_l = L_w^{set} - L_w$ and $e_f = W_{st} - W_{fw}$, respectively, where L_w is the measured water level and W_{st} , W_{fw} represent the steam and feedwater flow rates, respectively. The superscript N and set represent, respectively, the normalized value for the corresponding physical quantity and the set point value. In the FLC, both normalized errors, e_l^N and e_f^N , are fed firstly into the learning function and, from these normalized errors, the learning function creates and updates the rules of the fuzzy logic controller which is represented as w_i ($i = 1, \dots, 49$) in Fig.7. Based on these newly acquired control rules, the fuzzy logic controller performs the water level control, which results in the output value for the feedwater flow rate W_{fw} .

The SMU and LMU represent the steam flow and water level measurement units, respectively. The unit VPC means the valve position controller that moves the valve to the position that exactly corresponds to the feedwater flow rate from the fuzzy logic controller.

In the simulation test, the water level is assumed to be measured accurately and the feedwater flow rate is acquired from the output value of the fuzzy logic controller, assuming the VPC matches exactly the valve position to the commanded feedwater flow rate [9]. The noise signals in the steam flow rate are assumed to be Gaussian white noise whose magnitude is twice as high as the nominal value of the steam flow rate at 5% rated operating power. The number of data recorded for the input data of the wavelet transform is 64 samples which were sampled by the controller with the sampling time of 1 sec.

As can be seen in Fig.7, the measured value of the steam flow rate via SMU is stored in the last bytes, s_{63} , in the shift register denoted by S after all the data stored in S is shifted to the left. As for the actual input data for the wavelet transform, the samples in S are folded about the last s_{63} bytes, which results in a doubling of the recorded data samples in such a way that

$$D = \{d_0, d_1, \dots, d_{127}\} = \{s_0, s_1, \dots, s_{63}, s_{63}, \dots, s_1, s_0\}, \quad (12)$$

where d: data sample in the register D for the wavelet transform and s: data sample in the shift register S.

The reason for folding out of the samples of the steam flow rate measurements as in Eq.(12) is that, as you can see in section 3, the signal reconstruction or estimation is deteriorated at both boundaries, i.e., around the beginning and end positions. And so, we folded out the original samples to double the size where the value to be given to the controller is located at the center position of the input data of the wavelet transform.

With the aim of an on-line implementation, the maximum scale level is set to $J = 6$. The iteration number for the alternating projections is set to 40. After the removal of the

meaningless modulus maxima and the reconstruction of the wavelet transform by the alternating projections, the estimated signal is reconstructed from the inverse wavelet transform. The register D^E in Fig.7 represents these reconstructed samples. Among the samples in D^E , the average value for the two samples d_{63}^E and d_{64}^E is fed back to the error calculation module as a current value of the steam flow rate, i.e., $W_{st} = (d_{63}^E + d_{64}^E)/2$. When there is no variation in the steam flow rate, none of the modulus maxima are detected. In this case, the estimated value of the steam flow rate is given by $W_{st} = (S_{2,j}f(63) + S_{2,j}f(64))/2$, where S is the smoothing operator represented in Eq.(6).

In the simulation test, the FLC with the wavelet transform is applied to the steam generator model developed by Irving, et al [10]. With this model, we identified the tracking performance when the set point of the water level was varied from 0 to 100 mm at the control start and also investigated the disturbance rejection performance when the steam flow rate was increased at 2000 sec and decreased at 2500 sec, by 0.4 % of the rated steam flow rate [8]. For the existence of the measurement noise, the noise-corrupted steam flow rate is depicted in Fig.8. Fig.9 shows the level control performance of the FLC with the wavelet transform and the estimates of the steam flow rates are shown in Fig.10. As can be seen in Fig.9 and Fig.10, the FLC controls the water level stably under a very high noise environment, with the aid of the wavelet transform.

5. Conclusions

In this paper, a wavelet denoising method was described based on the wavelets proposed by Mallat and Zhong and a systematic way of noise discrimination was proposed for an efficient implementation. The wavelet denoising method was applied to the water level controller, where the wavelet transform generated the on-line estimation value of the steam flow rate within the sampling times. The fuzzy learning controller, used as a water level controller in this paper, with the wavelet transform showed a very satisfactory control performance for the water level control of the steam generators through the simulation test.

References

- [1] D. Gabor, "Theory of Communications", Journal of IEE, vol.93, pp.429~457, 1946.
- [2] M. Vetterli and C. Herley, "Wavelets and Filter Banks: Theory and Design", IEEE Transactions on Signal Processing, vol.40, no.9, pp.2207~2232, 1992.
- [3] S. Mallat and S. Zhong, "Characterization of Signals from Multiscale Edges", IEEE Transactions on Pattern Analysis and Machine Intelligence, vol.14, no.7, pp.710~732, 1992.
- [4] Z. Cvetković and M Vetterli, "Discrete-Time Wavelet Extrema Representation: Design and Consistent Reconstruction", IEEE Transactions on Signal Processing, vol.43, no.3, pp.681~693, 1995.
- [5] I. Daubechies, "Orthonormal Bases of Compactly Supported Wavelets", Communications on Pure and Applied Mathematics, vol.XLI, pp.909~996, 1988.
- [6] D. Belluzzo, M. Marseguerra, and S. Tarantola, "Wavelet Analysis of Fast, Short Lived

Transients with Noise”, SMORN VII, 7th Symposium on Nuclear Reactor Surveillance and Diagnosis, pp.176~184, June, Avignon, France, 1995

- [7] S. K. Menon and A. G. Parlos, “Gain-Scheduled Nonlinear Control of U-Tube Steam Generator Water Level”, Nuclear Science and Engineering, vol.111, pp.294-308, 1992.
- [8] G. Y. Park and P. H. Seong, "Application of Self-Organizing Fuzzy Logic Controller to Nuclear Steam Generator Level Control", Nuclear Engineering and Design, vol.167, no.3, pp.345~356, 1997.
- [9] A. Parry, J. F. Petetrot, and M. J. Vivier, “Recent Progress in SG Level Control in French PWR Plants”, Boiler Dynamics and Control in Nuclear Power Stations, pp.81~88, BNES British Nuclear Energy Society, London, 1985.
- [10] E. Irving, C. Miossec, and J. Tassart, "Toward Efficient Full Automation Operation of the PWR Steam Generator with Water Level Adaptive Control," Boiler Dynamics and Control in Nuclear Power Station, pp.309~329, BNES British Nuclear Energy Society, London, 1980.

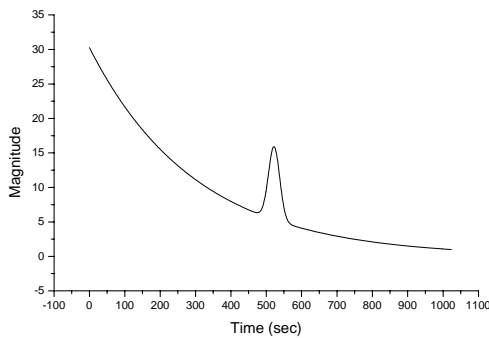


Fig.1 An original, arbitrary signal

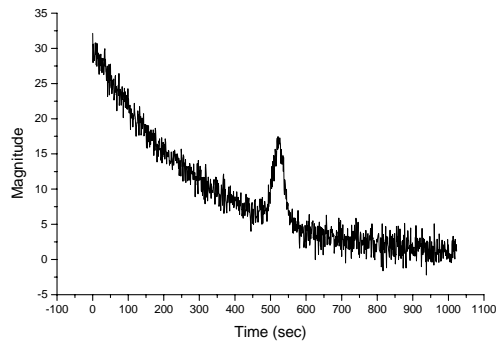


Fig.2 Signal with the Gaussian white noise

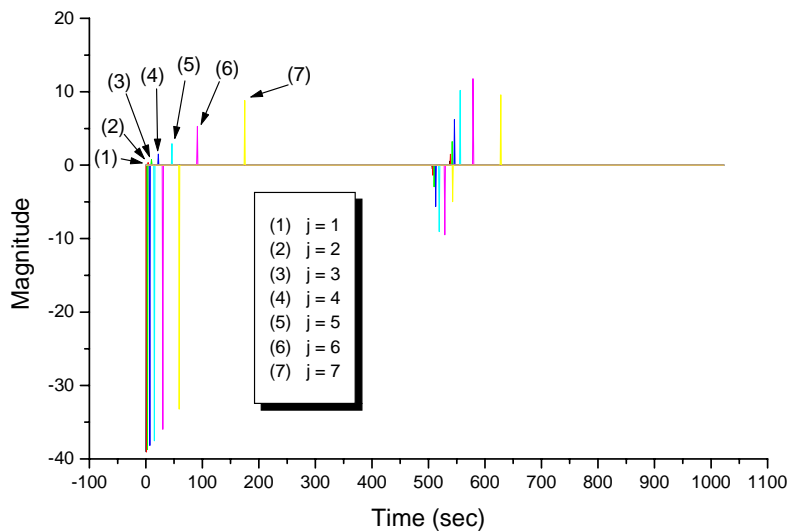


Fig.3 Modulus maxima for the pure signal

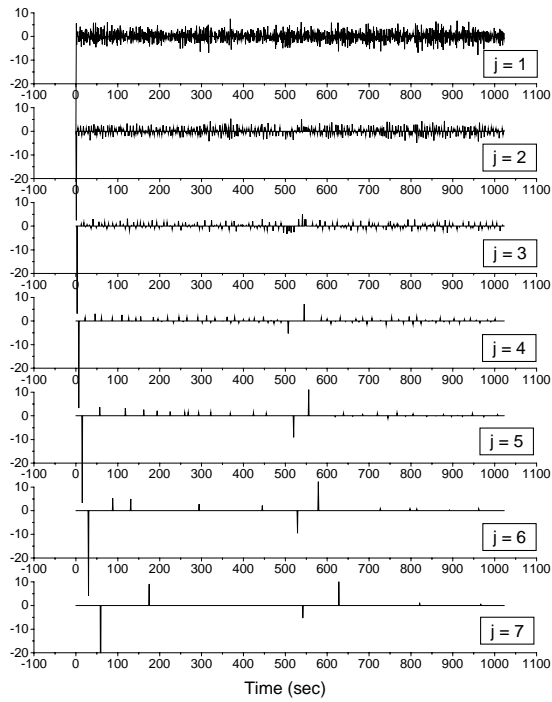


Fig.4 Modulus maxima for the signal with noise

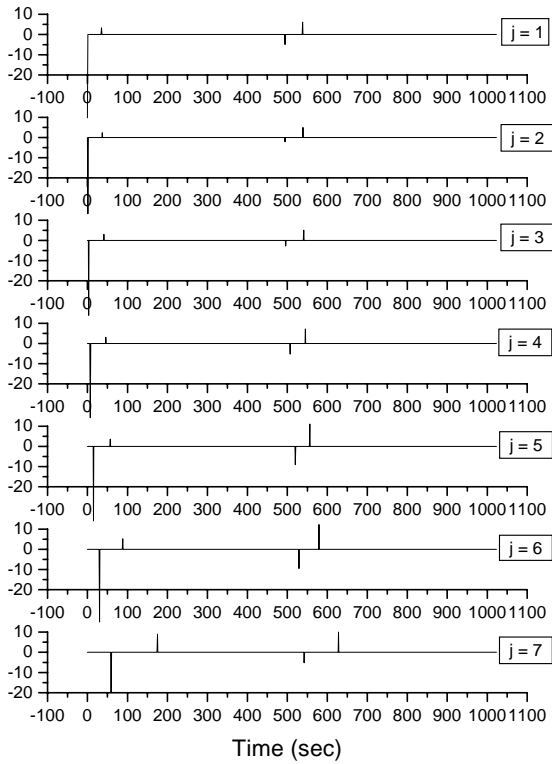


Fig.5 Results of discrimination for the modulus maxima

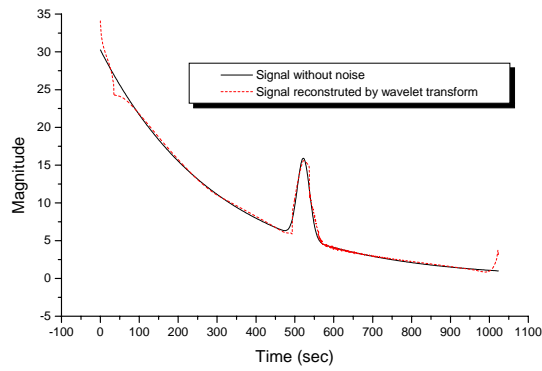


Fig.6 Reconstructed signal from the noisy signal

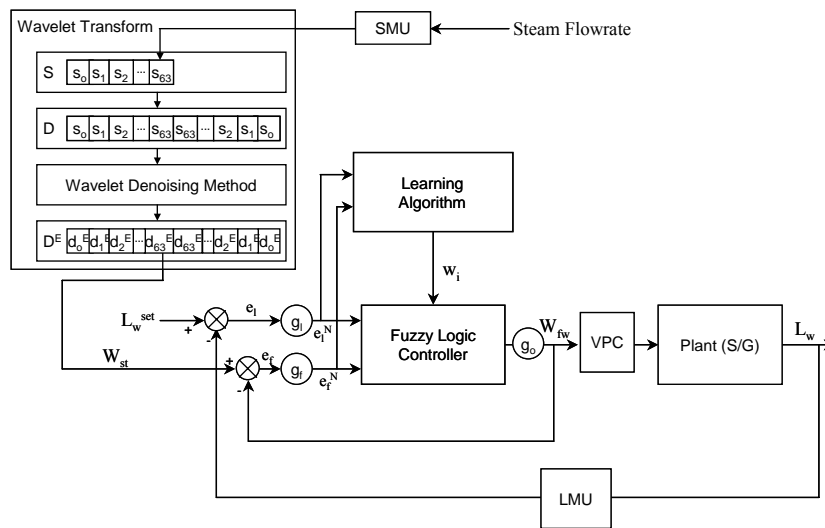


Fig.7 Schematic diagram of the FLC with the wavelet transform

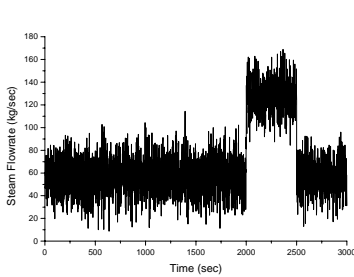


Fig.8 Noisy steam flow rate

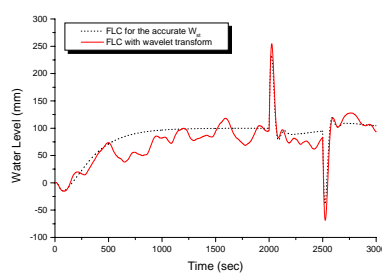


Fig.9 Result of FLC + WT at P = 5%&

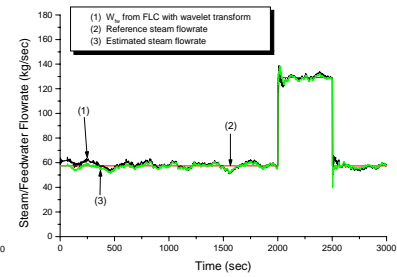


Fig.10 Estimated steam flowrate feedwater flow rates